Rev.Adv.Mater.Sci. 6 (2004) 1-6

MICROSTRUCTURE CONTROL OF Al_2O_3-ZrO_2 COMPOSITE BY FIBROUS MONOLITHIC PROCESS*

Taek-Soo Kim[1], Dong-Hwi Jang[1], Takashi Goto[2] and Byong-Taek Lee[1]

[1] School of Advanced Materials Engineering and Chungnam Research Center for Nano Materials, Kongju National University, 182 Shinkwan-dong, Kongju, Chungnam 314-701, Korea
[2] Institute for Material Research, Tohoku University, 2-1-1, Katahira, Aoba-ku, Sendai, Japan

Received: July 15, 2003

Abstract. Microstructure of alumina-zirconia composite was successively controlled using nanopowder and fibrous monolithic process. The microstructure was examined by back scattered electron microscope (BSEM) and Transmission electron microscope (TEM). As the passes of extrusion increase, the aligned size the $A1_2O_3$ and ZrO_2 particles were homogeneously reduced in accordance with equation of $D_{n-1}/R^{1/2}$, where D is an initial diameter of the feed rod and R is an extrusion ratio. The calculated and measured data agreed well. The Al_2O_3 fibers of about 4-6 μm were distributed within the monoclinic (m-) ZrO_2 matrix with an average thickness of about less than 2μm after four pass.

* Presented at International Conference Nanomaterials and Nanotechnologies (Crete, Greece, August 30-September 6, 2003)

1. INTRODUCTION

Al_2O_3 and ZrO_2 composite has been widely used in many industries, which requires strength [1], wear resistance [2], and corrosion resistance [3]. The excellent biocompatibility of the Al_2O_3-ZrO_2 composite expands its application area into total hip and joint prostheses and dental implants [4]. However, further application with reliability is limited due to an inherently low fracture toughness of the ceramic materials. Thus, modification of the brittle fracture mode has become a center of investigation. The typical examples of such modification were conducted using a mechanical alloying [5], sputtering [6], and spark plasma sintering [7], as well as a microstructural refining [8,9]. However, no remarkable success has been reported yet. Lately, coextrusion technique is newly introduced to fabricate a fiber type ceramic composite, and succeeded to combine a ductile manner in the brittle fracture behavior [10,11]. But, Kaya *et al*. [10] focused to sol-gel based technology, whereas Lienard *et al.* [11] to Si_3N_4 with submillimeter grains. Currently, Kim *et al.* [12] fabricated Al_2O_3-ZrO_2 composites by the coextrusion process, and obtained a successful refinement and homogeneous distribution of constituent phases.

In this investigation, microstructure of both Al_2O_3-ZrO_2 ceramic composites was controlled using the fibrous process and the resultant mechanical properties were examined. Present work describes a fabrication of fibrous Al_2O_3-ZrO_2 composites as well as a microstructure control technique. Resultant microstructure of the fibrous monolithic Al_2O_3-ZrO_2 composite was examined using back scattered electron microscope (BSEM) and transmission electron microscope (TEM).

2. EXPERIMENTAL

Powder mixtures of commercially used Al_2O_3 powder/polymer and ZrO_2 powder/polymer were prepared using a heated blender (C.W. Brabender Instruments, Inc., PL2000 Plasti-Corder with Roller Blade Mixing Heads). Average particle size of the starting materials is about 200 nm for Al_2O_3 (AKP-50, Sumimoto,

Corresponding author: Taek-Soo Kim, e-mail: taeksoo@kongju.ac.kr

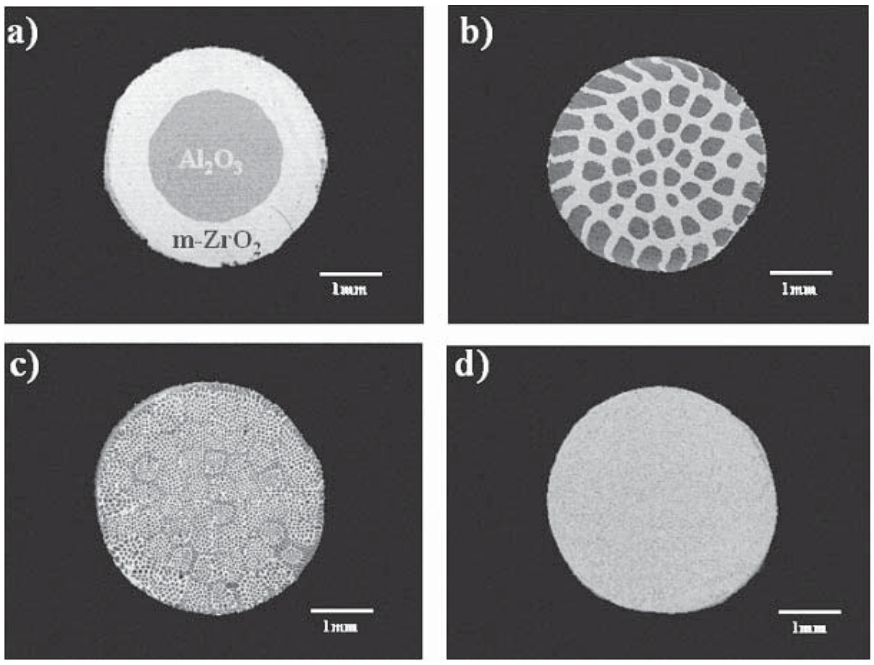

Fig. 1. SEM micrographs of the fibrous AP/ZP filaments with passes (a) first pass, (b) second pass, (c) third pass, and (d) fourth pass.

Japan) and 80 nm for ZrO_2 powder (Toso, Japan). The polymer was used as a binder of ceramics; it was Ethylene Vinyl Acetate (EVA) in granules (Elvax 250, Dupont). For lubrication during blending, stearic acid ($CH_3(CH_2)_{16}COOH$, Daejung chemicals & metals Co., Ltd) was added. The volume percent of the mixture was 50/50 for the Al_2O_3 powder/co-polymer and 40/60 for the ZrO_2 powder/polymer. In order to blend each powder with polymer, the mixing head and chamber of the blender were first heated to 130 °C using an oil type heating source and the EVA copolymer was added. After rotating the head for about 1-2 minutes, the ceramic powder was added slowly.

Mixtures of Al_2O_3/polymer (depicted as AP) and ZrO_2/polymer (depicted as ZP) were extruded into filament of 3.5 mm in diameter with an area reduction ratio of 70:1. However, the extrusion ratio was reduced to 55:1 from the second extrusion due to the area change on reloading. In order to make both phases into fibrous shape, AP was used for a core of about 21 mm in diameter, while ZP for an outer layer of about 3.4 mm in thickness, being 50:50 in vol.%. Each filament was reloaded in the extrusion die of 30 mm in diameter and reextruded, maintaining the composition of AP-50 vol.% ZP. This procedure was repeated until the third passed filament was obtained. The extrusion temperature and rate was 120 °C and 15 mm/min., respectively. Binder burn-out (BBO) of the filaments as extruded was carried out at 700 °C under flowing nitrogen atmosphere, and sintered at 1450 °C.

Microstructure and composition of the filaments were examined using Field Emission Scanning Electron Microscope (FE-SEM, JSM 6335F), Transmission Electron Microscope (TEM, EM2010) and Energy Dispersed Spectroscopy (EDS, Oxford 400). For TEM observation, sintered body was dimple grounded and ion-milled using a dimple grinder (Gatan Model656) and an ion miller Pips (Pips, Gatan).

3. RESULTS AND DISCUSSION

Fig. 1 shows a back scattered electron image of extruded AP/ZP composite with passes of extrusion. It is seen in Fig. 1a that AP forms in the shape of a fiber surrounded by ZP (white color), in which the diameter of the AP and thickness of ZP are about 2.16 mm and 1.49 mm, respectively. As the pass of extrusion increases, the microstructure becomes fine and homogeneous; the AP fiber is about 350 μm after second pass (b), while the microstructure in the last two filaments is not possible to measure. It is interesting for third passed bar to present a distribution of prior grains with about 0.3 mm in di-

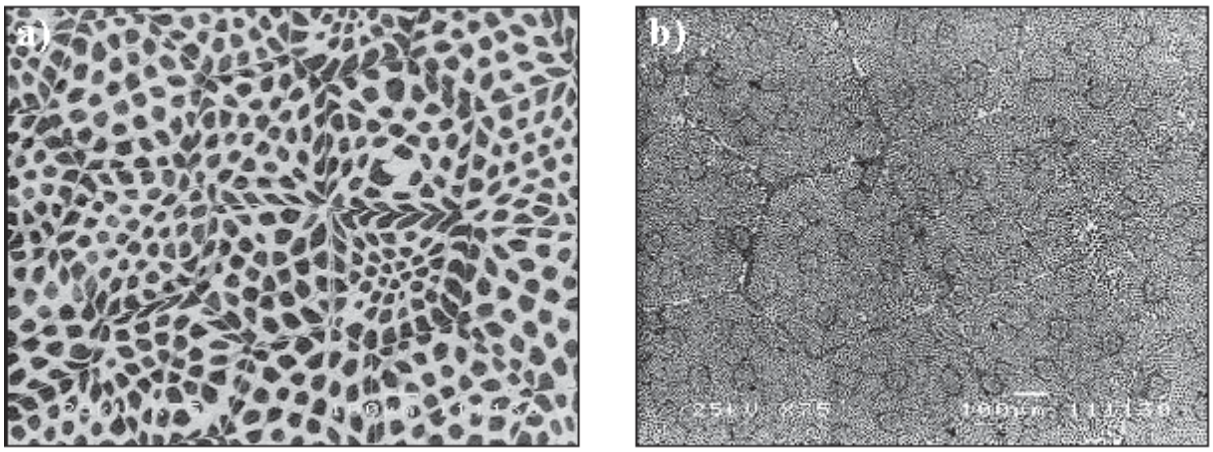

Fig. 2. SEM micrographs of fibrous AP/ZP filaments enlarged from Fig. 1 (c and d); (a) – third pass, (b) – fourth pass.

ameter. The prior grains maintain the microstructure of the second passed bar only with reduction of the area, corresponding to the extrusion ratio of 75:1. The 55 prior grains formed in the third filament are due to reloding the filaments of 55 ea. Continuing the process yields a homogeneous reduction in the particle size depending on the extrusion ratio.

Fig. 2 shows an enlarged SEM image taken from the third (a) and forth (b) filaments in Figs. 1c and 1d. The third filament consists of AP of about 45 μm in diameter, which is distributed within the prior grains of about 300-400 μm in diameter (a). It is seen that the size of the AP is almost homogeneous, but AP particles at the central part of each prior grain are more homogeneous than those at edge area. The difference in the microstructural alignment with the location die is possibly due to the difference in the plastic flow during the extrusion. Friction between AP and ZP becomes lower than that between AP (or ZP) and the die wall. The severe friction of the ceramic/polimer against the extrusion die results in reducing the quantity along with the surface of the resultant filaments. It also gives rise to the formation of abnormal pattern of

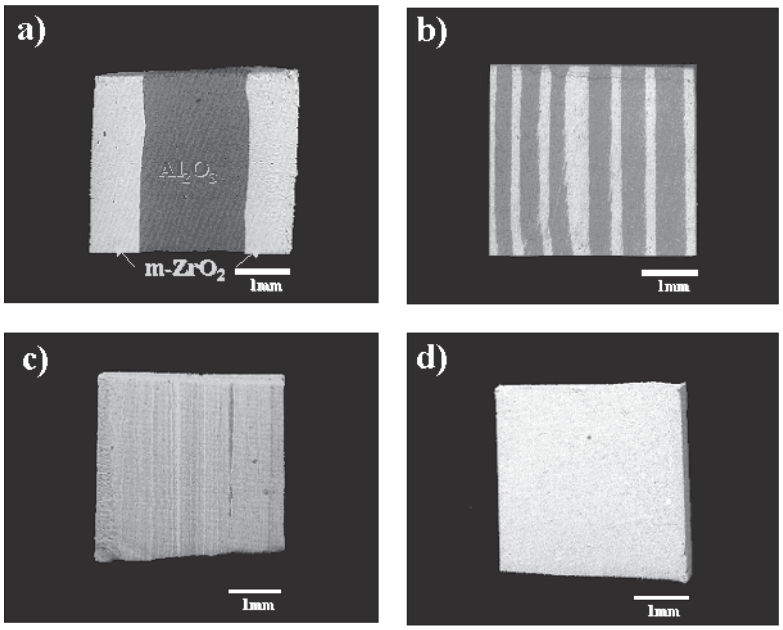

Fig. 3. SEM micrographs of the fibrous AP/ZP filaments with passes; (a) first pass, (b) second pass, (c) third pass, and (d) fourth pass.

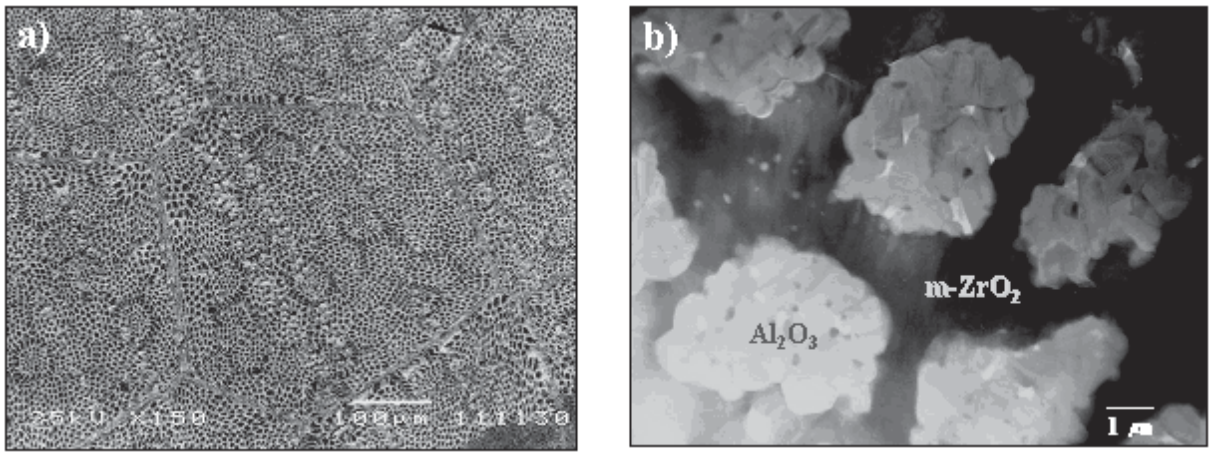

Fig. 4. (a) SEM and TEM (b) of the sintered Al_2O_3-ZrO_2 fibrous filament after 4th pass.

the AP/ZP alignment especially in the grain boundary area, resulting in a heterogenous microstructure along the prior grain boundaries. In order to overcome the problem in the microstructure, a use of lubricant will be much more effective than controlling the extrusion temperature and die angle, because the working temperature yields a drastic change in the viscosity of the polymer with a low melting temperature of 220 °C. In addition, the modification of the die angle will affect the extrusion force as well as a length of contact between the materials and the die. Thus, it is an easier way to use the lubricant rather than modifying the die angle and the extrusion temperature.

Further refinement in the microstructure can be obtained from the forth filament (see Fig. 2b). The homogeneous alignment of the fiber of AP (black color) less than 6 μm in ZP is also seen. Fig. 3 shows a SEM microstructure of the AP/ZP filament examined from the extrusion direction. The first filament presents a sound fibrous microstructure between AP (black) and ZP. With increasing in the pass of extrusion, the average diameter and the number of the fibers become fine and grow, as same as in Fig. 1 and Fig. 2, respectively.

In order to anticipate the microstructural change during the extrusion, the relationship between the mean diameter (D_n) of the fibers and the pass of extrusion was formulized as

$$D_n = D_n - 1/R^{1/2}, \quad (1)$$

where D_{n-1} is initial diameter of the feed rod, and R is an extrusion ratio. The equation indicates that the diameter of both the extruded bar and fiber varies only depending on the reduction ratio (R). This equation is very convenient for material engineer to anticipate the microstructural variation occurring during the fibrous monolithic process. The resultant size of the fibers obtained from the calculation and the measurement agreed well.

Figs. 4a and 4b show the sintered microstructure of forth filaments examined by SEM (Fig. 4a) and TEM (Fig. 4b), respectively. The sintered body reveals the same patterns of microstructure with the as-extruded filament (see Fig. 4a). Clear understanding of the microstructure of fibrous monolithic Al_2O_3/ZrO_2 sintered body follows from Fig. 4b. The white Al_2O_3 particles of about 4-6 μm are distributed within the black colored monoclinic (m-) ZrO_2 ma-

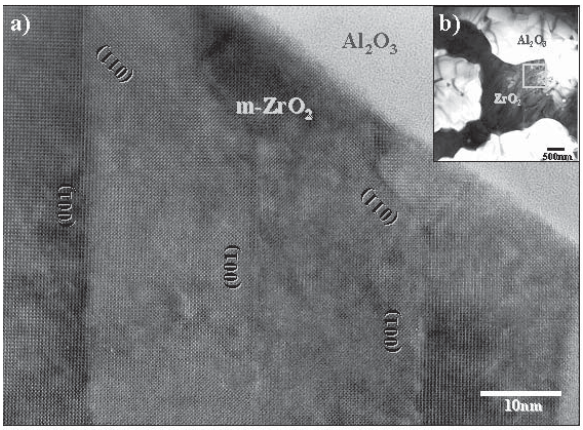

Fig. 5. (a) HRTEM and (b) TEM micrographs of the sintered Al_2O_3-ZrO_2 fibrous filament after 4th pass. (a) was enlarged from the square in (b).

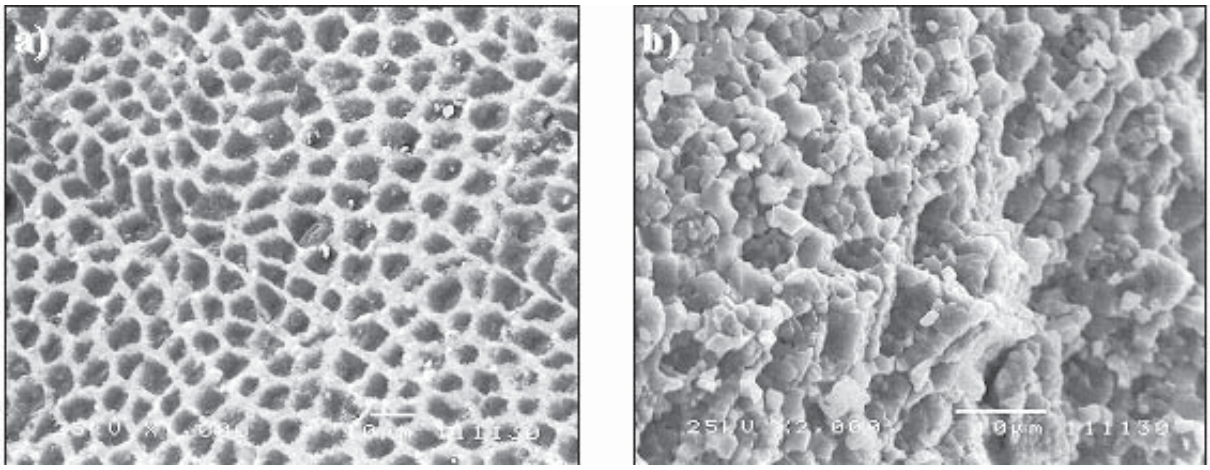

Fig. 6. SEM fractographs of the sintered Al_2O_3-ZrO_2 fibrous filament after 4th pass. (b) was enlarged from (a).

trix with an average thickness of about less than 2 μm. The homogenous distribution of the Al_2O_3 fiber within the ZrO_2 matrix will contribute to enhance the fracture toughness due to fibrous microstructure control.

Fig. 5 shows HRTEM image (a) taken from the Al_2O_3 and ZrO_2 phase boundary area (b) of the sintered forth filament. The ZrO_2 matrix contains mosaic type twins formed along the (100), (110) and (O11) phases.

SEM fracture surface of the forth filament obtained by a scattered electron mode is shown in Fig. 6. The fractography in Fig. 6a shows a homogeneous and fibrous monolithic distribution of Al_2O_3 (dark color) in ZrO_2 matrix. The fibrous Al_2O_3-ZrO_2 composite presents a network type fracture surface morphology and a little pulling-out-mode of Al_2O_3 fibers. The modified fracture mode corresponds to the homogenous distribution of fine Al_2O_3 fibers in ZrO_2 matrix. To sum up, the fibrous monolithic process regards as an efficient method for obtaining a homogenously distributed microstructure of ceramics. Further research on the effect of sintering conditions and composition in the fibrous monolithic Al_2O_3 and ZrO_2 composite may yield more fruitful mechanical properties.

4. CONCLUSION

Homogeneous Al_2O_3-ZrO_2 ceramic composite was successfully fabricated using a fibrous monolithic. As the passes of extrusion increased, the homogeneous distribution of the Al_2O_3 fibers in ZrO_2 matrix was formed, whereas the fiber size was reduced. The diameter of the Al_2O_3 fibers decreased from 2.50 mm after the first pass of extrusion, to 350 μm after the second pass, and then to 45 μm and 6 μm after the third and forth passes, respectively. The monolithic Al_2O_3-ZrO_2 composite presents a network type fracture surface morphology and a little pulling-out-mode of Al_2O_3 fibers.

ACKNOWLEDGEMENTS

This research was performed by the financial support of the 2002 NRL research program of Korean Ministry of Science and Technology.

REFERENCES

[1] S.C. Farmer and A.Sayir // *Engineering Fracture Mechanics* **69** (2002) 1015.
[2] A. Tarlazzi, E. Roncari, P. Pinasco, S. Guicciardi, C. Melandri and G.de Portu // *Wear* **244** (2003) 29.
[3] G. Heimke, P. Griss, G. Jentschura and E. Wemer, In: *Mechanical Properties of Biomaterials*, ed. by G. Hastings and A. Williams (Toronto, John Wiley & Sons, 1980) p. 207.
[4] D.R. Jrdan // *Ophthalmology Clinics of North America* **13** (2000) 587.
[5] N.H. Kwon, G.H. Kim, H.S. Song and H.L. Lee // *Mat. Sci. Eng. A* **299** (2001) 185.
[6] P. Gao, L.J. Meng, M.P. dos Santos, V. Teixeira and M. Andritschky // *Vacuum* **64** (2002) 267.
[7] G.D. Zhan, J. Kuntz, J. Wan, J. Garay and A.K. Mukheijee // *Scripta Mater.* **47** (2002) 737.

[8] X.-C.Yang and W. Reihemann // *Scripta Mater.* **45** (2001) 435.
[9] U. Betz, A. Sturm, J.F. Lofrlor, W. Wagner, A. Wiedenmann and H. Hahn // *Mater. Sci. Eng. A* **281** (2000) 68.
[10] C. Kaya, E. G. Butler and M. H. Lewis // *Journal of the European Ceramic Society* **23** (2003) 935.
[11] S.Y. Lienard, D. Kovar, R.J. Moon, K.J. Bowman and J.W. Halloran // *J. Mater. Sci.* **35** (2000) 365.
[12] G.H. Kim, T.S. Kim and B.T. Lee // *Korean J. Mater. Research* **13** (2003) 213.